GENERALIZED MEASURE OF VIBRATION EXPOSURE FOR HELICOPTER PILOTS

Aykut Tamer*, Andrea Zanoni†, Alessandro Cocco‡, Pierangelo Masarati§

Department of Aerospace Science and Technology,
Politecnico di Milano, Milano - Italy

*aykut.tamer@polimi.it †andrea.zanoni@polimi.it ‡alessandro1.cocco@mail.polimi.it, §pierangelo.masarati@polimi.it

Abstract

Helicopter pilots operate in a vibrating environment and the consequences vary depending on the affected body part. The usual method of evaluating the effects of vibration exposure is to calculate comfort levels as a result of whole body vibration. However, some other body parts are also adversely affected from vibration, such as hands and eyes, which in turn might degrade piloting quality. Therefore, a complete vibration assessment is necessary to reach a better estimation of pilot vibration exposure when comparing different configurations, tracking the changes during design and deciding on a safe flight envelope. This work presents a complete assessment by considering the vibrations on the seat surface, hand-grip of controls and vibration of the eye. As a result, the vibration measure includes comfort, handling and vision in a single formulation. The proposed measure is demonstrated by coupling a high-fidelity biodynamic pilot model to a helicopter aeroservoelastic model in a comprehensive simulation environment.

1 INTRODUCTION

Vibrations in rotorcraft are defined as the oscillatory response of the airframe to time dependent loads. The predominant sources of vibration are the forces and moments originating from the rotors, fuselage aerodynamics, engine and transmission. The resulting time dependent loads are transmitted to the fuselage, which excites the cockpit and the cabin, and consequently the crew and passengers. Sufficiently high level of vibrations cause physiological and psychological reactions in the human body [1]; helicopter pilot are not an exception. Additionally, pilots also have to operate the aircraft; hence, they are more affected by the adverse effects of vibrations than cabin crew and passengers. First of all, the short-term discomfort leads to more severe consequences in the long term, such as chronic pain [2]. Additionally, vibrations on control sticks can degrade handling qualities [3]; they may even cause closed loop instability [4] as a result of closed loop response. Finally, vibration degrades visual acuity due to eye motion [5] and vibration of the instrument panels. This can lead to increased reading errors and response times, thus degrading the display reading performance of the pilot.

Vibrations affect pilots globally at several body parts; hence, the common comfort ratings using whole-body vibration may not be sufficient. For this reason, this work proposes a generalized measure of vibration exposure in helicopter cockpit crew using a high-fidelity simulation environment. As shown in the sketchy pilot representation of Fig. 1, the measure involves:

- the whole body vibration measured at the seat interface ($\ddot{z}_s$), referred to as *comfort* vibration index (CVI);
- the vibration at the control stick grip ($\ddot{z}_c$), named as *handling* vibration index (HVI);
- the vibration of the eyes ($\ddot{z}_e$), designated as *visual* vibration index (VVI).

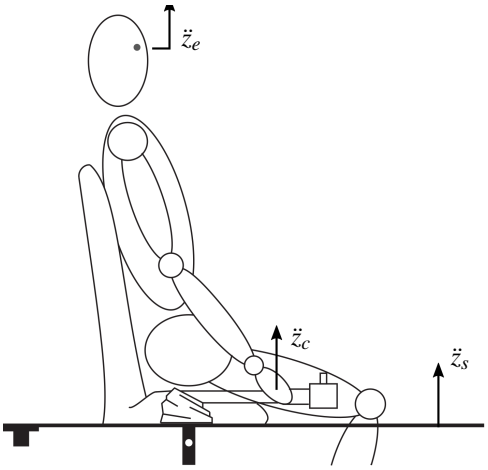

Figure 1: The three components of vertical acceleration considered in this study: the seat $\ddot{z}_s$, the grip of the collective stick $\ddot{z}_c$ and the pilot's eyes $\ddot{z}_e$.

The combination of the three above indices composes a generalized vibration index (GVI). Such a generalized formulation, within a framework for high-fidelity simulation, is believed to help tracking the effect of modifications made

Presented at the 45th European Rotorcraft Forum, Warsaw, Poland, 17-20 September, 2019

on the helicopter on the pilots' vibration exposure, including all significant aspects. As a result, the impact of vibrations on the occupational health of helicopter pilots and on the flight safety can be evaluated. This can be extremely helpful to engineers during the design phases of the vehicle, or when searching for the most effective vibration attenuation solutions for an existing design.

2 METHOD

This section explains how a generalized vibration index can be achieved for helicopter pilots. A conventional method is introduced first; then, the enhancement of the conventional method is explained.

2.1 Comfort Vibration Index

The conventional way of vibration assessment in vehicles is to measure or calculate the acceleration levels on the seat surface, where the body is in contact with the cushion. The accelerations can be calculated for a measured or computed excitation set. However, the perception of vibration is frequency and posture dependent. As a result, standards have been defined to guide comfort assessment: the rather general ISO-2631 [6], the air vehicle specific NASA Ride Quality (RQ) [7], and the rotorcraft specific Intrusion Index (II) from Aircraft Design Standard (ADS) 27-A [8].In Ref. [9], these standards were used for helicopter ride quality. It was concluded that the classical ISO-2631 better reflects the helicopter crew ratings than II or RQ. Starting from the discussion therein, the present work considers ISO-2631 as the framework for ride quality and revisits its critical aspects with regard to the characteristics of rotorcraft vibrations.

As recommended by ISO-2631, the measurement or computation should be made at the interface between the subject and the airframe. For most helicopter missions, this refers to the calculation of the translational accelerations [9] along three axes at the seat surface:

$$\mathbf{a}_{seat}(t) = \begin{bmatrix} a_{x,seat}(t) & a_{y,seat}(t) & a_{z,seat}(t) \end{bmatrix}^T \tag{1}$$

as a function of time t. However, since frequency weighting cannot be applied to a signal in the time domain, the Fourier series expansion ($\mathfrak{F}$) is performed:

$$\begin{bmatrix} A_x(\omega_n) \\ A_y(\omega_n) \\ A_z(\omega_n) \end{bmatrix}_{seat} = \frac{1}{T}\int_{-T/2}^{+T/2} \begin{bmatrix} a_x(t) \\ a_y(t) \\ a_z(t) \end{bmatrix}_{seat} \mathrm{e}^{-\mathrm{j}\omega_n t}\mathrm{d}t \tag{2}$$

with $\omega_n = n\Omega$, being $\Omega = 2\pi/T$ the fundamental frequency of a periodic signal of period T, where $A_{x,y,z}$ are the accelerations in the frequency domain. Then, after applying the frequency (W_d, W_k) and direction (k_x, k_y, k_z) weights defined in ISO-2631, the frequency weighted acceleration in time domain becomes:

$$\mathbf{a}_{w,seat}(t) = \sum_{n=-\infty}^{n=\infty} \begin{bmatrix} W_d(\omega_n)k_x A_x(\omega_n) \\ W_d(\omega_n)k_y A_y(\omega_n) \\ W_k(\omega_n)k_z A_z(\omega_n) \end{bmatrix} e^{\mathrm{j}\omega_n t} \tag{3}$$

In case of a dominant frequency ω, which is typical in rotorcraft [10], the weighted acceleration becomes:

$$a_{w,seat}(\omega) = \sqrt{(W_d k_x A_{x,\omega})^2 + (W_d k_y A_{y,\omega})^2 + (W_k k_z A_{z,\omega})^2} \tag{4}$$

which can be further simplified considering that the vertical component of the acceleration usually dominates:

$$a_{w,seat}(\omega) = \sqrt{(W_k k_z A_{z,\omega})^2} = W_k A_{z,\omega} \tag{5}$$

where W_k is shown in Fig. 2. The above mentioned weighted acceleration in terms of magnitude can be further averaged by considering its root-mean-square (RMS). In that case, a division by $\sqrt{2}$ is needed for tonal vibrations at specific frequencies, which is only a scalar factor, inessential within the scope of this work. As a result, we prefer to use signal amplitude in the remainder of this work. Then, the comfort vibration index (CVI) at a given frequency ω is defined as:

$$\mathrm{CVI}(\omega) = W_k A_{z,seat}(\omega) \tag{6}$$

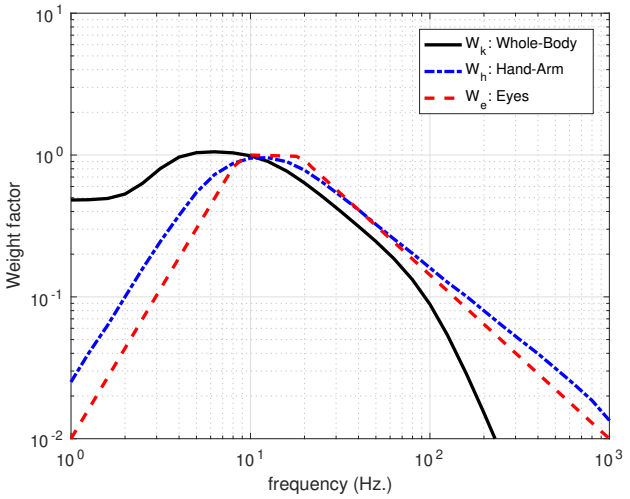

Figure 2: Frequency weights of vertical whole body vibration (W_k), hand-arm vibration (W_h) and eye vibration (W_e)

The analysis presented above can give insight into the comfort degradation as a result of the whole body vibration experienced by a passenger; but it only tells a partial story when the pilot is concerned. The next two sections describe the necessary additions to the conventional formula to achieve a generalized vibration measure of helicopter pilots.

2.2 Handling Vibration Index

The comfort vibration index considered in the previous section considers the motion of the whole-body, not specific body parts. While legs and feet are well supported on the seat and ground; arms and hands are connected to the

trunk via joints and therefore have more freedom to move as compared to former. Moreover, hands are prone to several vibration-related risks [11] and further can threaten flight safety if the hand motion is fed back to the controls [4]. Therefore it is beneficial to include the vibration of the hand in evaluating the effects of vibration on helicopter pilots.

In a conventional helicopter cockpit layout, the pilot is in vertical sitting posture and is supposed to control the vehicle through collective and cyclic control sticks. Both hands of the pilot hold grips of these sticks, which are connected to the airframe floor. Therefore, hands receive excitation from the floor through two paths: i) from seat to trunk and then to the arms and hands, ii) directly from the control stick. As a results, pilot hands are exposed to vibration. For the hands motion, there is no clear dominant direction; therefore the magnitude should be considered. Frequency weighting for human sensitivity to hand-arm vibration (W_h) is available in ISO-8041 standard [12] and presented in Fig. 2. Then, similar to the comfort vibration index of Eq. 6 a handling vibration index (HVI) can be given as:

$$\mathrm{HVI}(\omega) = W_h A_{hand}(\omega) \tag{7}$$

2.3 Visual Vibration Index

Considering the typical environment of a pilot resting in nearly vertical sitting posture, the whole body and instrument panel vibrate as a consequence of cabin floor and structure vibrations. The vibrations acting on the human body are transmitted to the skull through the spine, and from the skull to the eyes. Similarly, the displays are excited through an independent load-path. As a result, relative vibratory motion occurs between the eye and the visual displays. Increasing levels of vibration cause reading errors and longer response times, thus degrading the display reading performance of the pilot [5]. Either the vibration of the crew or that of the display screens can dominate the relative motion; however, it is likely that both contribute [13]. For both causes, the degradation is proportional to the amplitude of the vibration [14]. This work focuses on human biodynamic aspects of vibration assessment, therefore panel vibration is not considered.

In the case of involuntary motion of the superior body parts, such as the head and eyes, the identification of the dynamic response from measurements becomes more difficult. For this reason, the literature on eye response presents greater variability in the critical frequencies as compared to comfort-focused measurements on seat surface. Nevertheless, some of the data show similarities and has been confirmed by independent studies, thus allowing scientists to determine some trends. For example, results presented by Ohlbaum [15] suggest that the eye response, relative to the skull, starts increasing at about 12 Hz and shows a peak in the vicinity of 18 Hz; otherwise, it follows the skull with no noticeable amplification. Similarly, Ishitake [16] shows a maximum reduction of visual acuity at a frequency of 12.5 Hz. Collins [17] found the significant contribution of human biodynamics on visual performance degradation above 10 Hz. In a combined positive G manoeuvre and sustained vibration, 12 Hz is also reported as the target frequency for the effect of vibration on visual acuity [18]. The range for appreciable effects of vibration on visual performance is extended up to 31.5 Hz by Lewis and Griffin [19].

For the eye vibration, previous paragraph reports a high level of sensitivity between $12-18$ Hz., while remaining at significant levels until 30 Hz. Although there is no standardized frequency weighing for the eye vibration, these findings can be used to develop a sensitivity curve for the vibration of the eyes. In Fig. 2, the shapes of the whole-body and hand-arm frequency weights are similar: starting from a lower value, increasing up to unity near a highly sensitive frequency range and then reducing again. If a similar shape can be assumed with the reported sensitivity frequency intervals, we can achieve a frequency weighing for the eye as presented in Fig. 2. This frequency weight for the eye vibration (W_e) is multiplied by the acceleration of the eye and visual vibration index (VVI) is obtained:

$$\mathrm{VVI}(\omega) = W_e A_{eye}(\omega) \tag{8}$$

2.4 Generalized Vibration Index

We propose a generalized vibration index (GVI), which is composed of the indices described above: i) comfort vibration index (CVI), ii) handling vibration index (HVI) and iii) visual vibration index (VVI). These three are linearly summed with relative weights:

$$\mathrm{GVI} = \mathrm{c_C CVI} + \mathrm{c_H HVI} + \mathrm{c_V VVI} \tag{9}$$

where $\mathrm{c_C}, \mathrm{c_H}, \mathrm{c_V}$ are referred to as component weights and determines the relative importance of each components. The sum of the component weights are set to unity:

$$\mathrm{c_C} + \mathrm{c_H} + \mathrm{c_V} = 1 \tag{10}$$

As a result, the proposed GVI includes:

- acceleration estimates of the three components; namely the whole-body, the hand-arm and the eye;
- the frequency weights of these components determined by the standards or carefully conducted tests;
- component weights which allows to alter the formulation when needed.

3 ANALYSIS MODEL

This section explains how a detailed model is built to achieve a generalized vibration measure of helicopter pilots.

3.1 Helicopter Model

Three contributions to GVI require calculating the accelerations from the vibration source to human seat contact, hands and eyes. This could be achieved using an overall model which includes:

- high fidelity aeroelastic helicopter model for accurate vibratory loads estimation and transmission to the pilot seat;
- human biodynamics to involve amplification and suppression of vibrations as they propagate through the body;
- dynamically coupling the above two, i.e. human biodynamics and helicopter aeroelasticity.

MASST (Modern Aeroservoelastic State Space Tools), a tool developed at Politecnico di Milano, analyzes compact, yet complete modular models of linearized aeroservoelastic systems [20, 21]. In MASST, rotorcraft subcomponents are collected from well-known, reliable and state-of-the-art sources, assembled and glued together using the Craig-Bampton Component Mode Synthesis (CMS) method [22], and cast into state-space form. This approach is crucial to model helicopter subcomponents (rotors, airframe etc.) in their most suitable platforms and compose the overall model. In MASST, the assembled model is cast into a quadruple of matrices $\mathbf{A}$, $\mathbf{B}$, $\mathbf{C}$, $\mathbf{D}$ that define the system in state-space form:

$$\dot{\mathbf{x}} = \mathbf{A}\mathbf{x} + \mathbf{B}\mathbf{f} \tag{11a}$$

$$\mathbf{y} = \mathbf{C}\mathbf{x} + \mathbf{D}\mathbf{f} \tag{11b}$$

where vector $\mathbf{x}$ contains the states of the system, $\mathbf{y}$ is the system output, $\mathbf{f}$ includes the inputs. MASST interpolates the state-space model matrices in a generic configuration within the corresponding linear models evaluated in the space of prescribed parameters. In the Laplace domain, the model produces the input-output relationship:

$$\mathbf{y}(s) = \left[\mathbf{C}\left(s\mathbf{I} - \mathbf{A}\right)^{-1}\mathbf{B} + \mathbf{D}\right]\mathbf{f}(s) = \mathbf{G}(s)\mathbf{f}(s). \tag{12}$$

Therefore, MASST guarantees the success of a generalized vibration measure of helicopter pilots as follows:

1. flexibility in the source of sub-component formulation;
2. high-fidelity overall modeling through sub-component assembly;
3. capability of defining sensor-force relations between arbitrary structural points;
4. exporting proper models compatible for efficient evaluation of accelerations at selected positions as a result of defined inputs.

The high-fidelity helicopter model is built based on data representative of a generic, medium weight helicopter with an articulated 5 blade main rotor. A snapshot of the physical kinematic variables of the virtual helicopter model is shown in Fig. 3. The state-space model includes:

- rigid body degrees of freedom;
- flight mechanics derivatives of the airframe, estimated using CAMRAD/JA;
- elastic bending and torsion modes of the airframe extracted from NASTRAN, with 1.5% proportional structural damping superimposed in MASST;
- the first two bending and first torsion modes of the main and tail rotors including aerodynamic matrices in multiblade coordinates obtained using CAMRAD/JA;
- transfer functions of main and tail rotor servo actuators directly formulated in Matlab/Simulink, considering servo-valve dynamics and dynamic compliance [23];
- the nodes and coordinates for the sensors and the forces, directly defined in MASST.
- the biodynamic model is coupled to the high-fidelity helicopter model at the cockpit location.

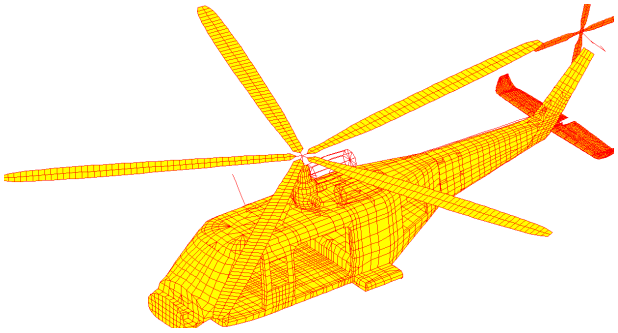

Figure 3: Snapshot of the virtual helicopter model.

3.2 Biodynamic Model

The accelerations on the seat surface, control stick grip and eye are required, as well as the interaction between pilot biodynamics and helicopter dynamics. Therefore, it is not sufficient to only measure the accelerations at the seat interface; the propagation of accelerations to the previously mentioned body parts is also necessary. For this purpose, a computational model is necessary to assess the crucial vibration characteristics.

The biodynamic modeling of human body is a recent import to helicopter analysis and therefore needs further attention. Human biodynamics can be modeled using Lumped-Parameter (LPM), Finite Element (FEM), and Multibody Dynamics (MBD) [24]. LPM uses masses, dampers and springs, to model the dynamics of the human body and is very common, thanks to its low computational cost and ease of parameter identification. The second one, FEM, is more useful than LPM for the analysis of vibration effects on isolated human organs such as the spine, since the flexibility of modeling and the resolution of the output is far richer. The MBD model is a good alternative for biodynamic analysis, considering its ability to model joints and

nonlinear elements [25]. MBD adds flexibility to LPM with the ease of constraint formulation, and can approach the capabilities of FEM with the formulation of flexible elements. Furthermore, multibody modeling can easily capture effects related to nonlinearities, especially those originating from 3D geometry, with ease.

As discussed in Ref. [26], the multibody dynamics approach is the most suitable for a coupled rotorcraft-pilot vibration assessment, especially when the upper body parts are involved in the analysis. Therefore, this work uses it to model the pilot's biodynamics. Within the scope of this work, a complete biodynamic model of the upper body as presented in Fig. 4, which is composed of the dynamics of spine-trunk, hand-arm, and eye, is necessary. The multibody model should be able to:

- be adapted to different human body types, since human mechanical properties can significantly vary within a population representative of helicopter pilots;
- easily change the posture, since the placement of control sticks and the seat configuration is not the same in different helicopters;
- provide a sufficiently high level of output resolution both in the spatial domain and in the frequency domain;
- be flexible in terms of building blocks.

A free, general-purpose multibody solver, MBDyn [27], developed at Politecnico di Milano[1], satisfies the above requirements with ease and efficiency, and hence it is selected as the biodynamic modeling environment.

3.2.1 Spine and Trunk

A multibody model of the human spine has been recently developed and presented in [26], which is based on a model originally proposed by Kitazaki and Griffin [28]. The model includes 34 rigid bodies associated with the section of the trunk corresponding to each vertebra from C1 to S1, and to 8 visceral masses. The relative displacement between each vertebral node is allowed only in the local z direction, which is assumed to lie in the direction locally tangent to the spine axis. The relative displacement in the x direction, which corresponds to the anatomical antero-posterior direction, and in the y direction, which corresponds to the anatomical medio-lateral direction, are constrained instead.

The vertebrae are interconnected by linear viscoelastic elements, acting on all the remaining, unconstrained degrees of freedom. The visceral masses are connected to the corresponding vertebrae: from T11 to S1, and between them, through linear viscoelastic elements.

The visceral part of the model is formed by 7 nodes, placed with an offset along the sagittal axis, from the T11 vertebra to the L5. They are linked to the corresponding vertebrae by a rigid element that constrains the three rotations and the displacement along the transverse axis; the displacement along the longitudinal and sagittal axes are constrained by linear viscoelastic elements.

The other lumped masses are placed in correspondence to the centers of the shoulder girdles, to account for the masses of the arms, of the pelvis and of the head. The last vertebra of the spine, S1, is connected to the cushion surface by viscoelastic elements representing the buttocks tissues. The node representing the buttock degree of freedom is constrained as to allow only the vertical relative displacement with respect to S1 and the rotation in the sagittal and coronal plane.

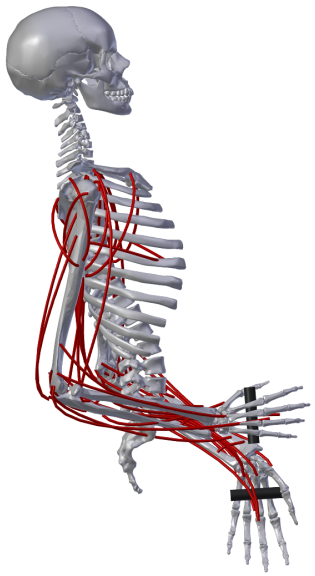

Figure 4: CAD representation of the human upper body.

3.2.2 Ocular Dynamics

The spine model explained in the previous section includes the motion of the head. However, there is an additional local motion between the head and the eye, which likely alters the involuntary motion of the eye; therefore causing the blurring perception of the displays. The ocular dynamics with respect to the head can be modeled using the same computational techniques that are used in biodynamic modeling (See for example Ref. [29]). However, transfer functions obtained from experiments are preferred at this stage, since cognitive processes intervene with the dynamical behaviour of eye. The complete dynamical modeling of ocular dynamics involving the cognitive interaction requires a dedicated biomechanical research and thus is beyond the scope of the present work. Therefore, the use of experimentally measured, empirical transfer functions of the eye has been selected to include the ocular dynamics, rather than completely ignoring its presence. Among the available studies, Ref. [30] is preferred, since it provides the head to

[1] `http://www.mbdyn.org/`, last retrieved in July 2019.

eye transfer function including magnitude, phase and their standard deviation. When the relative transfer function from head to eye is multiplied by the head acceleration of the spine-trunk model, the absolute acceleration of the eye is obtained. Comparison with a passive eye assumption is presented in Fig. 5.

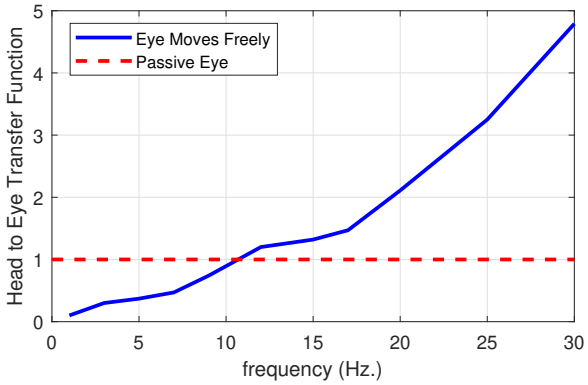

Figure 5: Head to eye transfer function

3.2.3 Hand-Arm

The multibody model of the upper limbs was initially presented in [25], based on the work proposed in [32], and subsequently improved in [33]. Each limb is composed of four rigid bodies that represent the humerus, the radius the ulna and the hand. The hand is represented by a single body: this simplification was made because the target simulations only involve grasping tasks.

The shoulder complex is not modeled in detail, disregarding the clavicle and the scapula. In fact, piloting tasks are typically performed with very low elevation angles of the humerus for both limbs; therefore, the expected effect of the scapula and clavicle motion on the shoulder kinematics is very limited.

The glenohumeral joint is represented by a spherical joint located at the glenoid fossa, removing 3 degrees of freedom. A revolute hinge represents the humeroulnar joint in correspondence to the center of the trochlea, allowing the rotation of the ulna with respect to the humerus only about the local lateral axis: this removes 5 degrees of freedom.

The humereroradial joint is represented by a spherical hinge, located at the humeral capitulum: it removes 3 degrees of freedom.

The proximal and distal radioulnar joints are modeled by single inline joint between a point P and the mechanical axis of the ulna. The position of point P is offset from the radius mechanical axis in the lateral direction: the offset is such as to leave the two bones' mechanical axes parallel when in the rest position, i.e. when the arms are extended anteriorly and the palms are facing upward. This joint removes 2 degrees of freedom.

At its distal end, the radius connects with the hand by means of a cardanic joint, allowing the wrist radioulnar deviation and flexion-extension rotations: this joint is composed by two simple hinges which have the axis rotated by 90. It removes 4 more degree of freedom.

In the end, the model has 7 degrees of freedom and its kinematics are underdetermined even when the motion of hand and shoulder is completely prescribed. For this model, a muscle-specific constitutive law was developed, based on the simplified Hill muscles model described in [32].

3.2.4 Combined multibody analysis

In order to connect the upper limb model to the seated spine model in MBDyn, a modal reduction of the spine model has been performed. This reduction is performed using the *boundary masses* approach proposed in [**?**]. To apply the method, the mass and stiffness matrix of the spine has been extracted; only the modes shapes in the sagittal plane have been considered. The contribute of the arms has been subsequently removed from the mass matrix of the spine: this term is now replaced by the total mass that is present in the upper limb model.

3.3 Pilot Seat

In a typical environment, a seat-cushion system provides the interface between the human body and the cabin floor. A properly designed interface can significantly alter and possibly reduce the vibrations received by the pilot. For this reason, a seat and cushion is adapted from a helicopter application [34]; it is described as a mass suspended by a spring and damper, as sketched in Fig. 6, with data reported in Table 1.

Table 1: Numerical values for the seat-cushion model.

	m_i (kg)	c_i ($\mathrm{N s m^{-1}}$)	k_i ($\mathrm{kN m^{-1}}$)
Seat	13.5[1]	750.00[1]	22.6[1]
Cushion	1.0[2]	159.00[1]	37.7[1]

[1]From Ref. [34]; [2]assumed

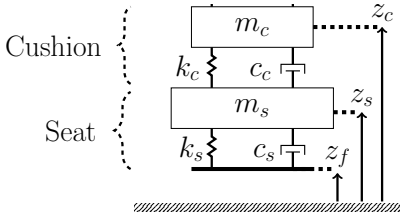

Figure 6: Cushion and seat model, providing interface between cabin floor and human body

4 RESULTS AND DISCUSSION

The detailed and fully coupled model described in the previous Sections is used to illustrate the benefits of using a generalized index for the vibration exposure of helicopter pilots. The analyses are conducted up to 30 Hz, since above

that frequency level the amplitude of vibratory loads typically reduce, and therefore they are not expected to cause significant consequences.

First, a comparison is made in Fig. 7. The conventional index (Section 2.1) is plotted against the generalized index (Section 2.4) with equal weight given to comfort, handling and visual contributions. Significant differences can be observed over the full range, except between 10 Hz – 20 Hz. On the other hand, the frequency values where the peaks are located are coincident. This suggests that within the frequency range of interest, the eye and hand-arm systems do not introduce additional resonances in the whole-body vibration. Instead, they amplify or dampen the vibrations transferred from the whole body dynamics to the hand and eye, depending on the frequency.

The second analysis shows the breakdown of the GVI of Fig. 7 into its contributions, namely comfort, handling and visual vibration indices. In Fig. 8, each contribution is shaded separately. In the low frequency region up to 5 Hz, the CVI dominates. Then, all three give more or less equal contribution up to 20 Hz, after which the visual contribution gains dominance. A benefit of this breakdown is the frequency-wise explanation of the differences between the conventional index and the generalized index that occurred in Fig. 7. Another practical use could be to choose the vibration reduction solutions more precisely, and target them to the most affected contribution. For example, when the CVI dominates, a global isolation of the airframe or the human body is more appropriate. On the other hand, if the VVI dominates as happened in this particular case beyond 20 Hz, the problem can be solved using the display modulation (see for example [35]), which is free of weight penalty.

The final analysis suggests further improvements to the GVI. A nominal GVI formulation, i.e. having prescribed component weights, makes it possible to compare vibration indices of different vehicle configurations. However, each component can have different priority and perception within a pilot population, and hence the sensitivity of the nominal GVI formula could be valuable. For this purpose, a robustness analysis can be made, as presented in the left plot of Fig. 9, which includes an area of possible values of GVI. The area is obtained by altering the weights given to CVI, HVI and VVI ensuring that the sum is always unity and then calculating the resulting GVI. The difference from the equal-weight case, which assumes a 1/3 weight for each contribution to the GVI, is remarkable. The two plots on the right provide the corresponding values of the constants for the maximum and minimum GVI values. In this particular problem, for example, when the GVI is maximum, the CVI dominates up to 14 Hz. Then, a narrow region is mainly influenced by the HVI; however, the GVI value is small and not sensitive to change in weights of the individual contributions. In the rest of the plot, beyond 17 Hz, the VVI leads the other two. Therefore, it can be stated that the equal-weight formulation is sensitive to CVI when the frequency is low, and to VVI when the frequency is high.

5 CONCLUSIONS

This work investigated the benefits of transforming the classical vibration assessment into a generalized vibration index (GVI). The suggested generalized formulation can be obtained in three steps:

- the acceleration contribution from the whole-body, hand-arm, and eye, namely the GVI contributions, are estimated in a coupled helicopter-human framework;
- frequency weights are applied to the value of mechanical acceleration of each GVI contribution;
- frequency weighted accelerations are linearly summed by adding another coefficient that reflects the importance of each GVI contribution.

Using a modular aeroservoelastic simulation framework, a coupled high-fidelity helicopter-human model was obtained, and the suggested GVI was demonstrated with its possible advantages over the classical one. It was found that:

- the GVI can be significantly different than the conventional assessment. Therefore, it can better reflect the adverse effects of vibrations on the pilot;
- hand-arm and eye vibration are directly related to the flight safety and can significantly contribute to the GVI; therefore, the GVI not only considers the comfort and health of the pilot, but also comprises safety;
- when the overall GVI is broken down into components, a risk assessment of vibration on the contributed human body parts can be made. As a result, a precise evaluation of vibration reduction techniques can be performed, depending on the frequency of the vibration source and the most affected body part at that frequency;
- a robust formulation can help to evaluate sensitivity of a prescribed GVI formulation to the contribution of each component.

The modular framework, which is used to obtained the overall high-fidelity analysis model, improves the GVI formulation. Future work is planned on improving the proposed GVI as follows:

- adding more contributions to the GVI, such as the vibration-induced strain of neck and spine;
- including nonlinear relations between the GVI contributions to the linear formulation.

The above mentioned extensions to the GVI require testing of helicopter pilots under realistic flight conditions. When the feedback about their feelings on the vibration exposure achieves a satisfactory level, a more accurate GVI formulation can be obtained.

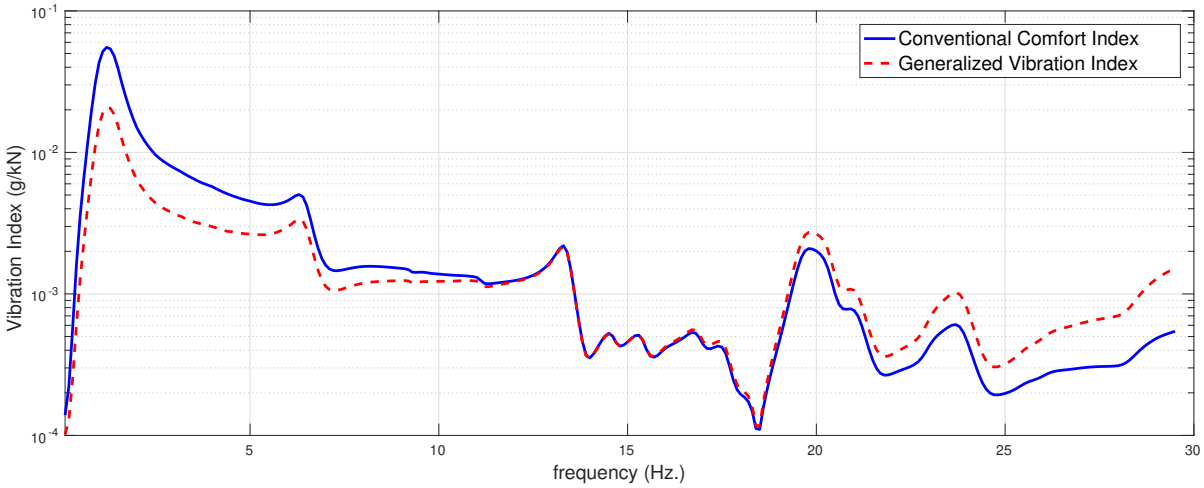

Figure 7: The proposed generalized vibration index, compared with conventional vibration exposure index for equal weights on comfort, handling, and visual vibration indices.

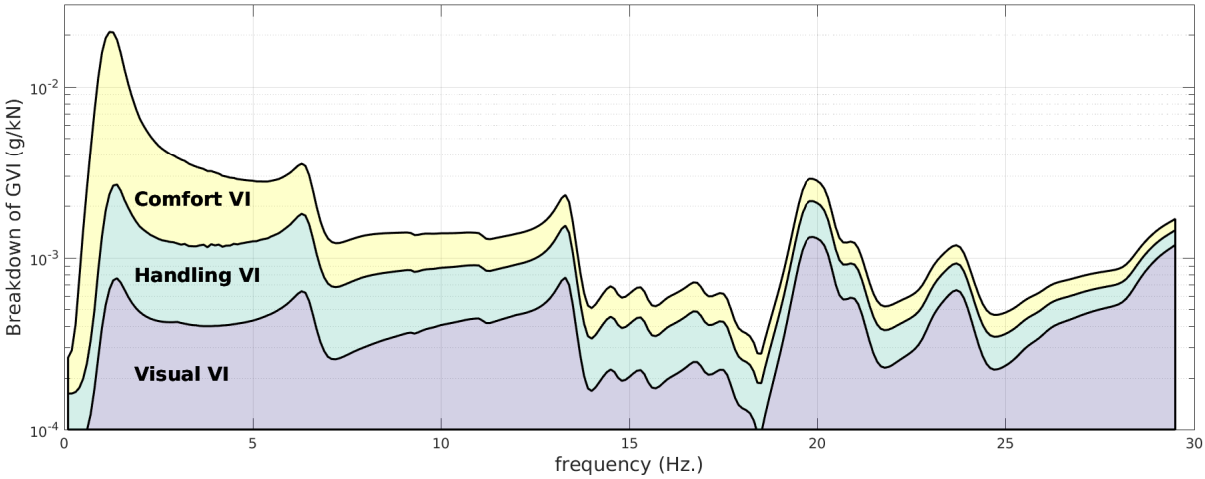

Figure 8: Component Breakdown of Generalized Vibration Index for equal weights on comfort, handling, and visual vibration indices.

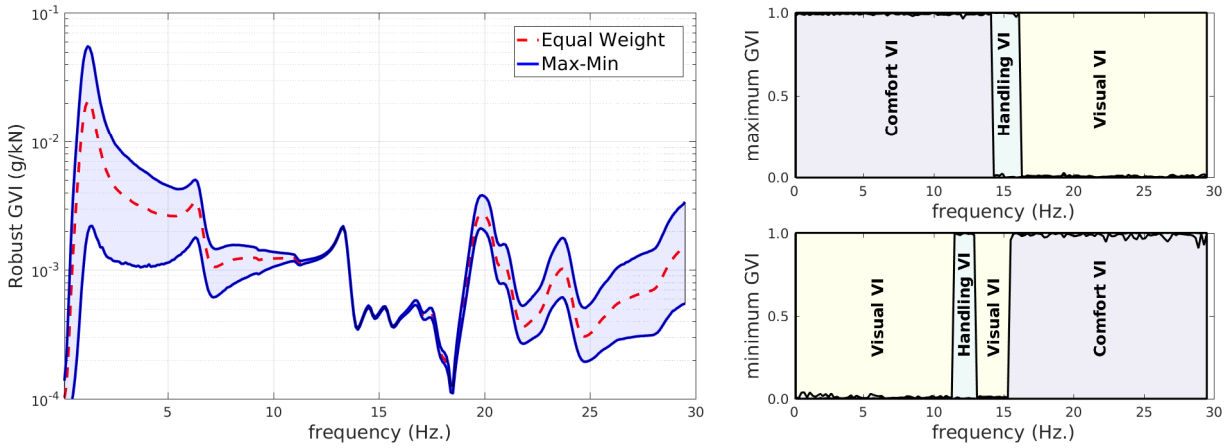

Figure 9: A robust generalized vibration index using different weights on comfort, handling, and visual vibration indices.

Copyright Statement

6 ACKNOWLEDGEMENTS

This work received partial support by Leonardo Helicopter Division. The authors acknowledge LHD for providing part of the data used in the analysis

References

[1] Jessica K. Ljungberg and Gregory Neely. Stress, subjective experience and cognitive performance during exposure to noise and vibration. *Journal of Environmental Psychology*, 27(1):44 – 54, 2007.

[2] Kristin L. Harrer, Debra Yniguez, Maria Majar Maria, David Ellenbecker, Nancy Estrada, and Mark Geiger. Whole body vibration exposure for MH-60s pilots. In *43th SAFE*, Utah, USA, 2005.

[3] Pierangelo Masarati, Giuseppe Quaranta, Massimo Gennaretti, and Jacopo Serafini. An investigation of aeroelastic rotorcraft-pilot interaction. In *37th European Rotorcraft Forum*, Gallarate, Italy, September 13–15 2011. Paper no. 112.

[4] Giuseppe Quaranta, Aykut Tamer, Vincenzo Muscarello, Pierangelo Masarati, Massimo Gennaretti, Jacopo Serafini, and Marco Molica Colella. Rotorcraft aeroelastic stability using robust analysis. *CEAS Aeronaut. J.*, 5(1):29–39, March 2014. doi:10.1007/s13272-013-0082-z.

[5] Michael J. Griffin. Eye motion during whole-body vertical vibration. *Human Factors*, 18(6):601–606, 1976.

[6] ISO. ISO mechanical vibration and shock - evaluation of human exposure to whole-body vibration. Technical Report ISO2631-1, ISO, 1997.

[7] Jack D. Leatherwood and Sherman A. Clevenson. A design tool for estimating passenger ride discomfort within complex ride environments. *The Journal of the Human Factors and Ergonomics Society*, 22(3):291–312, 1980.

[8] AMCOM. Requirements for rotorcraft vibration specifications, modeling and testing. Ads-27a, US Army AMCOM, 2006.

[9] Tobias Rath and Walter Fichter. A closer look at the impact of helicopter vibrations on ride quality. In *AHS 73rd Annual Forum*, Forth Worth, TA, USA, May 9–11 2017.

[10] Wayne Johnson. *Rotorcraft Aeromechanics*. Cambridge University Press, New York, 2013.

[11] N.J. Mansfield. *Human Response to Vibration*. Taylor & Francis, 2004.

[12] ISO. ISO human response to vibration-measuring instrumentation. Technical Report ISO8041, ISO, 2005.

[13] Ann Nakashima and Bob Cheung. The effects of vibration frequencies on physical, perceptual and cognitive performance. Technical Report DRDC Toronto TR 2006-218, DRDC Toronto, October 2006.

[14] Charles R. O'Briant and Morton K. Ohlbaum. Visual acuity decrements associated with whole body plus or minus gz vibration stress. *Aerospace Medicine*, 41(1):79–82, 1970.

[15] Norton K. Ohlbaum. *Mechanical Resonant Frequency of the Human Eye in Vivo*. PhD thesis, Aerospace Medical Research Laboratory, 1976.

[16] Yuzo Miyazaki Tatsuya Ishitake, Hideo Ando and Fumika Matoba. Changes of visual performance indced by exposure to whole-body vibration. *Kurume Medical Journal*, 45:59–62, 1998.

[17] Allan M. Collins. Decrements in tracking and visual performance during vibration. *Human Factors*, 15(4):379–393, 1973.

[18] Mary K. Kaiser Robert S. McCann Leland S. Stone Mark R. Anderson Fritz REnema Wiliam H. Paloski Bernard D. Adelstein, Brent R. Beutter. Influence of combined whole-body vibration plus g-loading on visual performance. Technical Report NASA-TM-2009-215386, NASA, May 2009.

[19] CHRISTOPHER H. LEWIS and MICHAEL J. GRIFFIN. Predicting the effects of vibration frequency and axis, and seating conditions on the reading of numeric displays. *Ergonomics*, 23(5):485–499, 1980.

[20] Pierangelo Masarati, Vincenzo Muscarello, and Giuseppe Quaranta. Linearized aeroservoelastic analysis of rotary-wing aircraft. In *36th European Rotorcraft Forum*, pages 099.1–10, Paris, France, September 7–9 2010.

[21] Pierangelo Masarati, Vincenzo Muscarello, Giuseppe Quaranta, Alessandro Locatelli, Daniele Mangone, Luca Riviello, and Luca Viganò. An integrated environment for helicopter aeroservoelastic analysis: the ground resonance case. In *37th European Rotorcraft Forum*, pages 177.1–12, Gallarate, Italy, September 13–15 2011.

[22] Roy R. Craig, Jr. and Mervyn C. C. Bampton. Coupling of substructures for dynamic analysis. *AIAA Journal*, 6(7):1313–1319, July 1968.

[23] Herbert E. Merritt. *Hydraulic Control Systems*. John Wiley & Sons, New York, 1967.

[24] Navid Mohajer, Hamid Abdi, Saeid Nahavandi, and Kyle Nelson. Directional and sectional ride comfort estimation using an integrated human biomechanical-seat foam model. *Journal of Sound and Vibration*, 403:38 – 58, 2017.

[25] Pierangelo Masarati, Giuseppe Quaranta, and Andrea Zanoni. Dependence of helicopter pilots' biodynamic feedthrough on upper limbs' muscular activation patterns. *Proc. IMechE Part K: J. Multi-body Dynamics*, 227(4):344–362, December 2013. doi:10.1177/1464419313490680.

[26] Aykut Tamer, Andrea Zanoni, Vincenzo Muscarello, Alessandro Cocco, Giuseppe Quaranta, and Pierangelo Masarati. Biodynamic modeling techniques for rotorcraft comfort evaluation. *Aerotecnica Missili & Spazio*, June 2019.

[27] Pierangelo Masarati, Marco Morandini, and Paolo Mantegazza. An efficient formulation for general-purpose multibody/multiphysics analysis. *J. of Computational and Nonlinear Dynamics*, 9(4):041001, 2014. doi:10.1115/1.4025628.

[28] Satoshi Kitazaki and Michael J. Griffin. A modal analysis of whole-body vertical vibration, using a finite element model of the human body. *Journal of Sound and Vibration*, 200(1):83–103, February 1997. doi:10.1006/jsvi.1996.0674.

[29] P. Pascolo, R. Carniel, and S. Grimaz. Dynamical models of the human eye and strabismus. *Chaos, Solitons & Fractals*, 41(5):2463 – 2470, 2009.

[30] R. A. Lee and A. I. King. Visual vibration response. *Journal of Applied Physiology*, 30(2):281–286, 1971.

[31] Andrea Zanoni, Pierangelo Masarati, and Giuseppe Quaranta. Upper limb mechanical impedance variability estimation by inverse dynamics and torque-less activation modes. In P. Eberhard and P. Ziegler, editors, *2nd Joint International Conference on Multibody System Dynamics*, Stuttgart, Germany, May 29–June 1 2012.

[32] E. Pennestrì and R. Stefanelli. Linear algebra and numerical algorithms using dual numbers. *Multibody System Dynamics*, 18:323–344, 2007. doi:10.1007/s11044-007-9088-9.

[33] P. Masarati, G. Quaranta, and A. Zanoni. A detailed biomechanical pilot model for multi-axis involuntary rotorcraft-pilot couplings. In *41st European Rotorcraft Forum*, Munich, Germany, September 1–4 2015.

[34] Young-Tai Choi and Norman Wereley. Biodynamic response mitigation to shock loads using magnetorheological helicopter crew seat suspensions. *Journal of Aircraft*, 42(5):1288–1295, 2005.

[35] Mary K. Kaiser, Bernard D. Adelstein, Mark R. Anderson, Brent R. Beutter, Albert J. Ahumada Jr., and Robert S. McCann. Stroboscopic image modulation to reduce the visual blur of an object being viewed by an observer experiencing vibration, April 2014. US Patent No: 8,711,462.